Materials Science Forum Vol. 157-162 (1994) pp. 1379-1386

X-RAY TEXTURE ANALYSIS IN FILMS BY THE REFLECTION METHOD: PRINCIPAL ASPECTS AND APPLICATIONS

D. Chateigner, P. Germi and M. Pernet

Laboratoire de Cristallographie, CNRS, BP 166, F-38042 Grenoble Cédex 09, France

Keywords: Film Texture Analysis, Defocusing Correction, High-T_c Superconductors

ABSTRACT

We review the principal characteristics of defocusing correction in thin films texture analysis using the Schulz reflection technique. Consequences are examined on $YBa_2Cu_3O_7$ films compared to classical bulk-like corrections. Principal effects are revealed in the high tilt angle region and, for highly oriented films ($YBa_2Cu_3O_7$ films on MgO), the film-like corrections offers better precision on the quantitative evaluation of the different parts of the texture than the bulk-one.

INTRODUCTION

Texture analysis of polycrystalline compounds have been proved of great interest to explain physical properties of materials, especially if these latter are highly anisotropic. A random distribution of crystallite orientations giving oftenly averaged physical properties, the texturation is needed to improve them for optimal utilizations. The characterization of the resulting textures is consequently of crucial importance. Numerous methods have been employed to improve the texturation either of powdered bulk samples (rolling, uniaxial pressure, magnetic alignment, crystalline growth ...) or thin film compounds (laser ablation, sputtering, chemical vapour deposition ...). In the case of the Schulz reflection method [1] (which we use in our experiments) these two kinds of samples have to be considered differently since the irradiated volumes do not evolve identically. Thin films texture analysis using this method provides more informations than classical experiments like rocking curves or φ-scan procedures. This technics gives information from the total thickness of the film, but the usual intensity corrections have to be modified for taking into account the enhancement of the irradiated volume during the tilt of the sample. We remind here the principle of intensity corrections for defocusing in the case of thin films in view to establish the true pole figures.

The recent development of high Tc superconductors has given rise to a great interest in their texture analysis, particularly for thin films in order to connect a preferred crystallographic orientation to physical properties. On the other hand we show how we can estimate the relative proportion of the principal textures existing in $YBa_2Cu_3O_7$/MgO superconducting samples from the operated corrections.

EXPERIMENTAL

The texture analyses have been realized with a Courbon S.A. (S^t. Etienne) texture sample holder mounted on a horizontal θ-2θ goniometer (GMI-Grenoble). We use the $Cu_{K\bar{\alpha}}$ radiation supplied by a Rigaku RU300E rotating anode which offers up to 60kVx300mA in power. The incident beam is monochromatised by the (002) reflection of a flat graphite (Huber-Rimsting) specimen of 0.4° mosaïc spread, which is essential for the study of thin films deposited on single crystalline substrates [2]. The beam is collimated by two crossed slits of 0.84mm large and 0.6mm high. The diffracted line is detected through a horizontal slit of 1mm by an Inel proportionnal counter. The signal is finally filtered by an SCA Ortec tension switcher before the data are collected in a Compaq 386/20 computer. The correction and pole figure layout is realized with a Compaq 486/50 computer using our own programs (Cortexg, Phiscan and Pofint) written in Turbo Pascal 5.5.

Since we currently observe strong textures in oxide films [3] the step angles choosen for the pole figure scans have to be small (0.5° or less), in view to avoid wrong interpolated intensity levels. Consequently isointensity lines are not useful and we draw direct pole figures where only experimental points are represented. The studied samples have been elaborated by MOCVD at LMGP-Grenoble (YBCO films). This technic is well described elsewhere [4].

The randomly oriented bulk sample of $YBa_2Cu_3O_7$ (YBCO) has been synthezised by classical solid state reactions starting with the 97% pure oxide powders (Y_2O_3, BaO and CuO). The random orientation of the resulting powders has been controled by comparing their θ-2θ spectrum with the theoretical ones. The agreement was satisfactory, by less than 2% of difference for the majority of the peaks below θ=40°. The defocusing curves realized on these samples were measured by integrating the diffracted intensity during one rotation of the sample around its normal, φ, for each tilt position, χ. The orthorhombic symmetry with 3.82Å x 3.88Å x 11.67Å unit cell parameters of $YBa_2Cu_3O_7$ implies a great number of neighbouring peaks. Consequently a relatively thin aperture of the detecting slit is needed and we recorded the defocusing curves with a high counting time of several minutes for each χ position to improve the statistics (in order to get precisely peak and background curves at high χ values).

THEORETICAL BACKGROUND

In the following we develop the useful expressions for the correction of pole figures in the case of Schulz reflection technics for the study of thin compounds. On our diffractometer the value χ=0° is define when the φ axis is colinear with the diffraction vector, **k**, and χ=90° when **k**⊥φ. For high enough χ values it is well known that defocusing occurs causing an intensity loss by peak broadening and irradiated surface increasing [5,6]. Usually this effect is corrected by the experimental set up of defocusing curves obtained from bulk samples whithout preferred orientation [7]. Such samples are generally feasible, and offer the possibility to correct pole figures up to χ≈80°. On the other hand, making untextured thin compounds is practically impossible, even on polycrystalline or amorphous substrates [8,9]. Such undesired textures can be promoted by interaction with the substrate (particularly with well matched interfaces) or the result of anisotropic growth speed of the crystallites. De facto, it becomes impossible to correct pole figures made on films. One solution consists in an analytical correction of the data using the experimental bulk defocusing curves. This means that the calculated curves for layers are available with the same experimental arrangement and material as for the bulk.

Films

Wenk & al. [10] proposed for the first time a formulae adapted to the correction of single layer deposited on substrates, based on the previous work of Schulz, and applied it to polycrystalline films

of silicon. We take again here this formulation which gives the defocused intensity of the film, $I^f(\chi)$, from the one of the bulk, $I^b(\chi)$:

$$\frac{I^f(\chi)}{I^b(\chi)} = 1 - \exp\left(\frac{-2\mu T}{\sin\theta\cos\chi}\right) \qquad (1)$$

Here θ is the Bragg angle of the considered (hkl) reflection, T and μ are respectively the thickness and the linear absorption coefficient of the film.
Due to the exponential term the defocusing curve of the film does not content a constant region for its low χ part , like the bulk generally exhibits. In addition we can remark that the allowable domain of the pole figure is extended in the high χ region since the irradiated volume increases with χ.

Substrates

If the substrate is crystalline, it would be interesting to study the influence of its texture on that of the layer. Here also, the pole figures cannot be corrected directly like a simple bulk (uncovered) since there is an absorption of both incident an diffracted beam into the film. We proposed recently the following expression for the correction [11] :

$$\frac{I^s(\chi)}{I^{bs}(\chi)} = \exp\left(\frac{-2\mu T}{\sin\theta_s\cos\chi}\right) \qquad (2)$$

$I^s(\chi)$ and $I^{bs}(\chi)$ are respectively the defocused intensity of the covered and uncovered substrate, while θ_s is the Bragg angle for the considered peak of the substrate.
Since the absorption of the beam increases with χ, the pole figure is less extended on its periphery than for an uncovered bulk.

Multilayers

The particular physical properties of multilayer compounds had given interest in the microscopic and macroscopic comprehension of their structure, where texture analysis may play an important rule of characterization. By combining equations (1) and (2), we can refine the appropriate correction form needed in this analysis. For a multilayer, the j^{th} layer from the top of the sample is diffracting an intensity, $I_j(\chi)$, which has to be corrected by :

$$\frac{I_j(\chi)}{I_j^b(\chi)} = \left[1 - \exp\left(\frac{-2\mu_j T_j}{\sin\theta_j\cos\chi}\right)\right] \exp\left(\frac{-2\sum_{i=1}^{j-1}\mu_i T_i}{\sin\theta_j\cos\chi}\right) \qquad (3)$$

$I_j^b(\chi)$ is the bulk defocusing curve for the material constituting the j^{th} layer at the Bragg angle θ_j. The indice i entering the summation refers to all the layers which are deposited on top of layer j, and the summation represents the absorption along these layers. The principal requirement here is the obligation to analyse a peak which is sufficiently separated from the others.

From (3) we can deduce the correction formulae for different types of multilayers. Let us consider the most current type, which consists of two kinds of materials, A and B, deposited J times one AB unit on the other periodically stacked (means $T_A=T_B$). We call this compound $(AB)_J$ multilayer. The first deposited layer is B (interface) and the last is A (top of the sample). In such configuration, equation (3) gives :

$$\frac{I_A(\chi)}{I_A^b(\chi)} = K_A(\chi)\left(1 + \sum_{i=1}^{J-1}\exp\left[\frac{-2i(\mu_A T_A + \mu_B T_B)}{\sin\theta_A\cos\chi}\right]\right) \qquad (4)$$

and

$$\frac{I_B(\chi)}{I_B^b} = K_B(\chi) \sum_{i=1}^{J} \exp\left[\frac{-2[i\mu_A T_A + (i-1)\mu_B T_B]}{\sin\theta_B \cos\chi}\right] \qquad (5)$$

$$\text{with} \qquad K_X(\chi) = 1 - \exp\left(\frac{-2\mu_X T_X}{\sin\theta_X \cos\chi}\right) \qquad (6)$$

Here X refers to the considered phase A or B. The b exponent denotes the bulk defocusing curve of the X phase. Pursuing for more general cases, we can obtain the correction expression for three or more different layers in each unit of the stack. If the stack unit is composed by K different layers, and deposited J times, with k in the intervall [A..K], we can write :

$$\frac{I_X(\chi)}{I_X^b(\chi)} = K_X(\chi)\left(\delta_X + \sum_{i=1}^{J-\delta_X} \exp\left[\frac{-2}{\sin\theta_X \cos\chi}\left(i\sum_{k=1}^{x-1} \mu_k T_k + (i-1+\delta_X)\sum_{k=x}^{K} \mu_k T_k\right)\right]\right) \qquad (7)$$

with $\delta_X=1$ if k=1 and $\delta_X=0$ for k>1.

For sufficiently thin layers (relatively to the linear absoption coefficient) the exponential term can be developped and the $K_X(\chi)$ coefficient can be replaced by [12] :

$$K_X(\chi) = \frac{-2\mu_X T_X}{\sin\theta_X \cos\chi} \qquad (8)$$

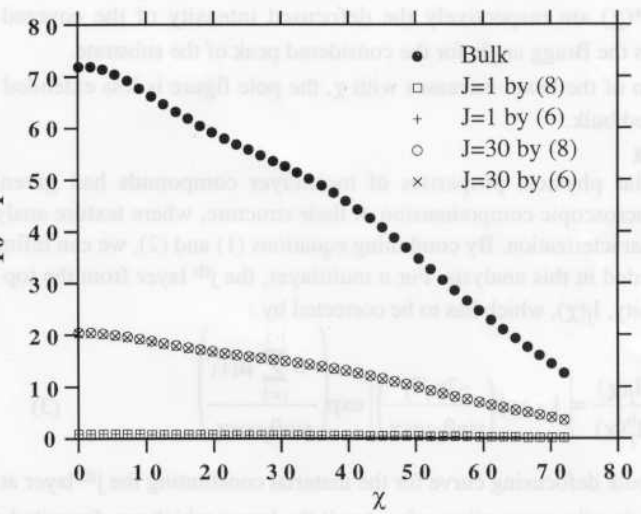

Fig.1 : Defocusing curves for the (103) reflection of the YBaCuO phase at θ=16.44° for an YBCO/YSZ multilayer sample. The layer type curves have been calculated through the equations (6) and (8) for two number of deposited AB unit, J=1 and J=30. The thicknesses of the layers are 50Å for both YBCO and YSZ phases and we calculated $\mu_{YBCO}=0.10915\mu m^{-1}$ and $\mu_{YSZ}=0.06667\mu m^{-1}$.

A comparison between the employment of (6) and (8) is made on figure 1 in the case of a YBCO/YSZ multilayer sample, for J=1 and J=30. The thickness of the two phases are 50Å and we made the calculation for the (103) reflection of YBCO. The linear absorption coefficients are $\mu_{YBCO}=0.10915\ \mu m^{-1}$ and $\mu_{YSZ}=0.06667\ \mu m^{-1}$. The two formulations (6) and (8) give defocusing curves in very good agreement in this case.

The increase in number of (AB) units, J, tends rapidly to the same defocusing as for bulk, and consequently needs an identical correction. On figure 2 are represented the correction curves,

$I(\chi)/I(0)$, of the same sample as figure 1. We clearly see that for ten AB units and more, these curves are quite identical for the experimental bulk and for the calculated one. However this effect is lowered for thicker layers and higher μ coefficients.

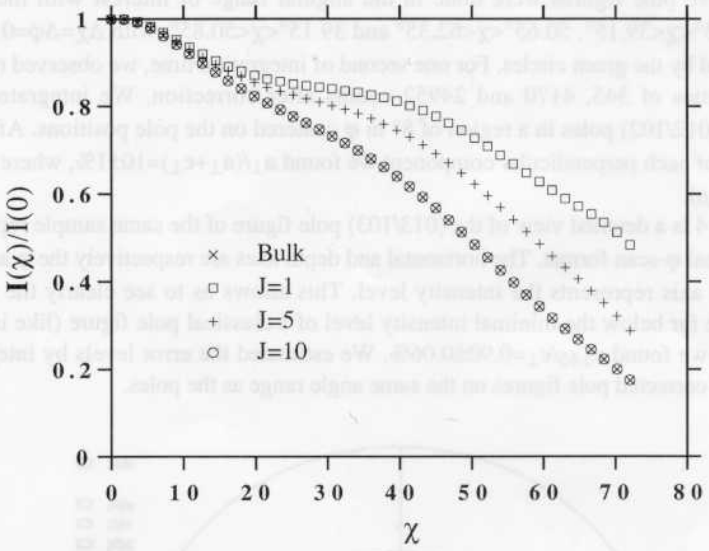

Fig.2 : Correction curves for the (103) reflection of the YBCO phase of the same sample as in figure 1. The number of deposited (AB) units is increasing. The calculated curves are given for J=1, 5 and 10 and are compared to the experimental bulk one. Notice the quite similar evolution of the bulk curve and for J=10.

EXAMPLES

Single crystalline MgO substrates take an important place in high temperature superconductor realizations because they exhibit a relatively low dielectric constant, and due to their cheapness in front of other possible single crystals. Deposited on such substrates, the YBCO phase shows physical properties comparable to the best one when the texture of the film is strong. The studied samples all exhibit critical temperatures over 85K, with transition width less than 2K. On such substrates the texture is characterized by **c** axes of the crystallites oriented perpendicularly to the substrate plane, and with the **a** and **b** parameters epitaxially aligned with MgO unit cell parameters (this texture is called $\mathbf{c}_{\perp 0}$). In such configuration one of the essential physical property, the critical current density Jc, can flow in the **ab** planes where it is about ten time greater than along the **c** axis. On the other hand Jc is greatly affected by misoriented crystallites which cause high angle grain boundaries [13,14]. Two types of misorientations can be easily produced in the case of MgO substrate. The first type, $\mathbf{a}_{\perp}$, corresponding to **a**-axis perpendicular to the surface, depends principally of the substrate temperature during the deposition. This orientation (with the $\mathbf{b}_{\perp}$ component) is well revealed by the examination of the (102/012) pole figure. The second type corresponds to $\mathbf{c}_{\perp}$ crystallites rotated by $\varphi°$ around **c** from the principal direction ($\mathbf{c}_{\perp\varphi}$) the most current occuring with φ=45°. This misorientation is explained by the formation of a near coincidence site lattice (NCSL) [15,16] between YBCO and MgO named Σ'=8 referring to the MgO lattice, and is shown by studying the (013/103) pole figure. The better statistic of the (013/103) diffraction compared to (012/102) made us choose the former for the evaluation of $\mathbf{c}_{\perp 45}$. Figure 3 is a multipole

figure of the (012/102) $\mathbf{a}_\perp$ and $\mathbf{c}_\perp$ component (θ=13.90°), and (013/103) reflections (θ=16.35°) of a 2200Å thick film of YBCO on MgO, respectively delimited on the figure by the inner, outer and middle ring. Since only the (00l) and (h00) peaks appeared on the θ-2θ scan realized on this sample, the three respective pole figures were done in the angular range of interest with the following parameters : 27.45°<χ<39.15°, 50.65°<χ<62.35° and 39.15°<χ<50.85°, with $\Delta\chi=\Delta\varphi$=0.45°. These zones are delimited by the green circles. For one second of integration time, we observed respectively maximum intensities of 345, 4170 and 24952 counts after correction. We integrated the total intensities of the (012/102) poles in a region of 8° in φ centered on the pole positions. After average on the four poles of each perpendicular component we found $\mathbf{a}_\perp/(\mathbf{a}_\perp+\mathbf{c}_\perp)$=10±1%, where $\mathbf{c}_\perp$ denotes the sum ($\mathbf{c}_{\perp 45}+\mathbf{c}_{\perp 0}$).

The figure 4 is a detailed view of the (013/103) pole figure of the same sample represented in a three dimensionnal φ-scan format. The horizontal and depth axes are respectively the φ and χ angles while the vertical axis represents the intensity level. This allows us to see clearly the $\mathbf{c}_{\perp 45}$ poles placed in this case far below the minimal intensity level of a classical pole figure (like in figure 3). After integration, we found $\mathbf{c}_{\perp 45}/\mathbf{c}_\perp$=0.90±0.06%. We estimated the error levels by integrating the empty parts of the corrected pole figures on the same angle range as the poles.

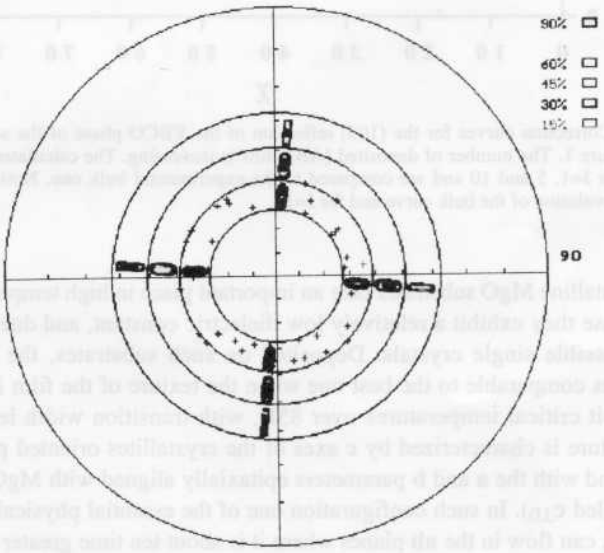

Figure 3 : Multipole figure of the (012/102)$\mathbf{a}_\perp$, (012/102)$\mathbf{c}_\perp$ and (013/103) reflections (resp. inner, outer and middle ring) of a 2200Å thick YBCO film on (100)MgO. θ=13.90° (012/102) and θ=16.35° (013/103). Note the presence of an important part of $\mathbf{a}_\perp$ oriented crystallites. (012/102)$\mathbf{a}_\perp$: Imax=345 cts, (012/102)$\mathbf{c}_\perp$: Imax=4170 cts and (013/103) : Imax=24952 cts.

It is clear that an accurate correction of the pole figures has to be carried out before to give quantitative appreciations of the relative parts of the texture. For samples with such strong textures the differences between film and bulk-like corrections are first sensitive on the maximal intensity value and consequently on the integrated ratios.

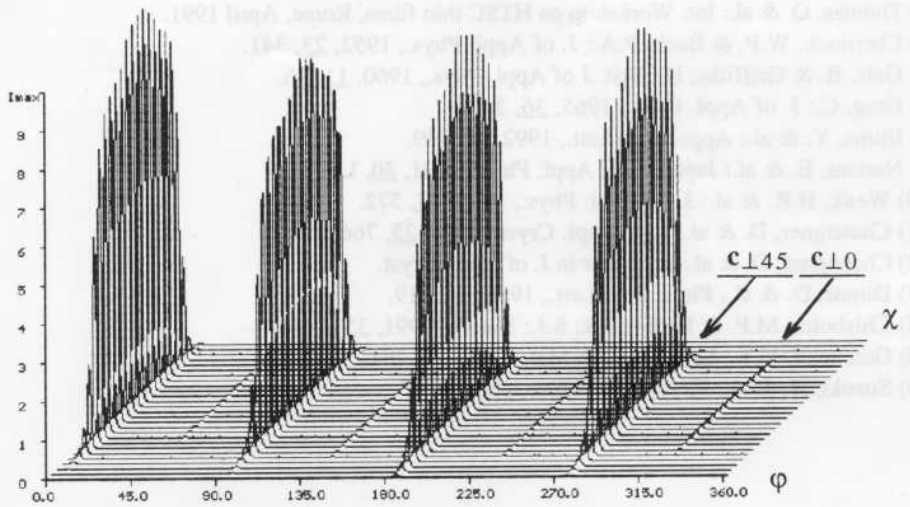

Figure 4 : Three dimensionnal φ-scan representation of the (013/103) pole figure of the fig.3. The $\mathbf{c}_{\perp 45}$ component is clearly visible. $39.15° < \chi < 50.85°$, $\Delta\chi = \Delta\varphi = 0.45°$. Green lines defines every 2.25° in χ.

For example, bulk-like corrections on the previous YBCO sample gives $\mathbf{a}_\perp/(\mathbf{a}_\perp+\mathbf{c}_\perp)=9\pm2\%$ and $\mathbf{c}_{\perp 45}/\mathbf{c}_\perp=1\pm0.15\%$. While average value of the ratios are slightly shifted down and up respectively, both errors are doubled. The maximal intensities of the (012/102)$\mathbf{a}_\perp$, (012/102)$\mathbf{c}_\perp$ and (013/103) pole figures increase from the previously found values up to 454, 6155 and 36096 cts respectively. Of course more differences between film and bulk-like corrections are observed in $I_{max.}$ for higher χ's, i.e. (012/102)$\mathbf{c}_\perp$ component. These effects are increasing with the thickness of the layer.

CONCLUSION

The texture studies of various thin compounds can be ruled out if particular corrections for defocusing and absorption are accomplished. We have detailed these later in some of the most current configurations of thin samples. Their application have been proved efficient for the quantitative determination of the principal components of the texture in highly textured YBCO films analyses. The effect of film-like corrections is more sensitive as the tilt angle becomes higher. In the case of multilayers we have shown that the correction to be applied becomes identical to the bulk one after some deposited unit.

ACKNOWLEDGEMENTS

The Alcatel-Alsthom industry is greatly acknowledged for its partial support in the thesis work of one of us (D. Chateigner). We also wish to thank C. Dubourdieu from the LMGP-Grenoble who provided the sample.

REFERENCES

1) Schulz, L.G.: J. of Appl. Phys., 1949, 20, 1030.
2) Wenk, H.R.: J. of Appl. Cryst., 1992, 25, 524.
3) Pernet, M. & al.: EMRS-92 proceedings, J. of All. & Comp., 1993, 195, 149.

4) Thomas, O. & al.: Int. Workshop on HTSC thin films, Rome, April 1991.
5) Chernock, W.P. & Beck, P.A.: J. of Appl. Phys., 1952, 23, 341.
6) Gale, B. & Griffiths, D.: Brit. J of Appl. Phys., 1960, 11, 96.
7) Feng, C.: J. of Appl. Phys., 1965, 36, 3432.
8) Iijima, Y. & al.: App. Phys. Lett., 1992, 60, 769.
9) Narumi, E. & al.: Japan. J. of Appl. Phys., 1991, 30, L585.
10) Wenk, H.R. & al.: J. of Appl. Phys., 1990, 67, 572.
11) Chateigner, D. & al.: J. of Appl. Cryst., 1992, 25, 766.
12) Chateigner, D. & al.: to appear in J. of Appl. Cryst.
13) Dimos, D. & al.: Phys. Rev. Lett., 1988, 61, 219.
14) Chisholm, M.F. & Pennycook, S.J.: Nature, 1991, 351, 47.
15) Gertsman, V.Y.: Scrip. Met. & Mat., 1992, 27, 291.
16) Suzuki, H. & al.: Physica. C, 1990, 190, 75.